SLS Note 16/97
October 1997

Error Estimates of Injection Magnets

C H Gough
A Streun

PSI

Error Estimates of Injection Magnets

C H Gough / A Streun

1. Introduction

Top-up operation of the SLS Storage Ring may require novel and stringent tolerances on the time and amplitude errors of the pulsed field waveforms of the injection magnets, so that the X-ray experiments are not disturbed. This Note gives practical estimates of the error limits for these magnets. Errors are either changes from the nominal for the kicker magnets, or changes from zero for the leakage field for the septum magnet.

The SLS Storage Ring has kicker magnets, K1 to K4, placed symmetrically in an 11m-long straight section, as shown in Fig.1 (attached to end of note). The choice of four magnets with identical deflections was made so that identical current waveforms would give identical magnet conductor heating, and identical remanence; this would minimise the closed orbit kick during top-up. The straight section is free from quadrupoles, so the deflection bump is not dependant upon the machine optics. A large straight section (about 11.5m) is to be used, so reducing the deflection needed from K1-K4.

For brevity, an equation which is valid in both the horizontal x-direction and the vertical z-direction uses the variable y.

2. Injection error

Fig.2 shows an idealised horizontal bump (exaggerated in size, since the displacement is only about 15mm in an 11m length), with the circulating beam arriving from the left and leaving to the right. There is a transit time (of the order of 30nsec) for the electrons to pass from K1 to K4, but in this Note, this transit time (or time skew) is ignored.
The four deflection pulses have a time function $f\,(t)$ and an amplitude

$$\theta_{i0:}\ \theta_i(t) = \theta_{i0}\cdot f\,(t).$$

The time dependancy is not explicitly written, only θ_i. The angles θ are signed values, positive for clockwise; θ_1 and θ_4 are positive, θ_2 and θ_3 are negative. The corresponding angles φ are in the vertical plane, and should in theory be zero at all times; in practice there will be a small component which has an important effect.

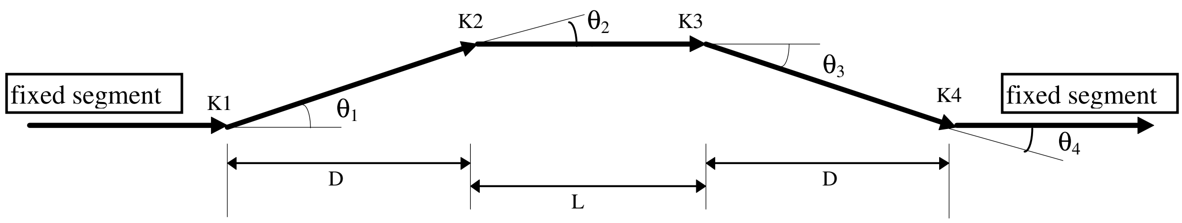

Fig.2 Horizontal geometry of storage ring bump.

2.1 Single turn injection error

In Fig.2, the circulating beam must traverse the two fixed segments for perfect orbit closure, but the three segments in between are not fixed. In Fig.3a-b are shown (in very exaggarated form), two families of bumps that will still give perfect orbit closure.

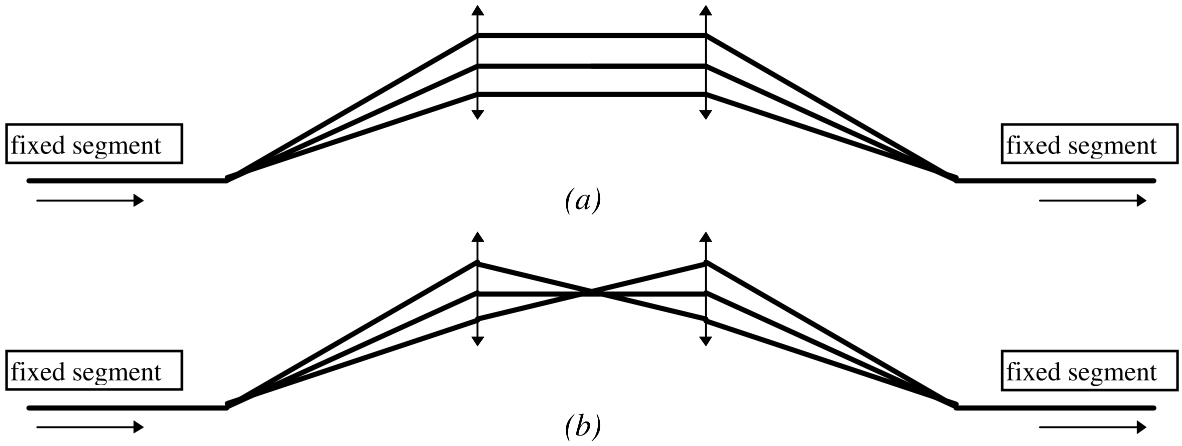

Fig.3 Family of symmetric (a) and aysmmetric (b)angle errors, still giving orbit closure.

The (signed) angles should sum to zero, and the difference is the Angle Error. The Displacement Error is conveniently measured at the centre of the injection straight (at location s_c relative to an arbitrary origin), since this is a point of symmetry of the lattice:

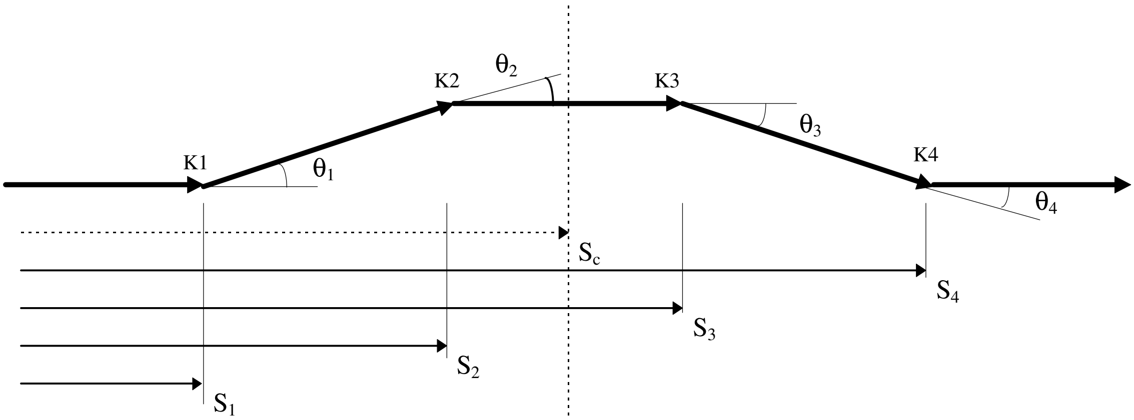

Fig.4 Horizontal geometry of storage ring bump.

The transformation of the four kicks to the centre of the injection straight is obtained by successive application of drift space transfer matrices:

$$\begin{pmatrix}\Delta x\\ \Delta x'\end{pmatrix}_c=\begin{pmatrix}1 & s_c-s_4\\ 0 & 1\end{pmatrix}\cdot\left\{\begin{pmatrix}0\\ \theta_4\end{pmatrix}+\begin{pmatrix}1 & s_4-s_3\\ 0 & 1\end{pmatrix}\cdot\left\{\begin{pmatrix}0\\ \theta_3\end{pmatrix}+\begin{pmatrix}1 & s_3-s_2\\ 0 & 1\end{pmatrix}\cdot\left\{\begin{pmatrix}0\\ \theta_2\end{pmatrix}+\begin{pmatrix}1 & s_2-s_1\\ 0 & 1\end{pmatrix}\cdot\begin{pmatrix}0\\ \theta_1\end{pmatrix}\right\}\right\}\right\}$$

$$\Rightarrow\quad \begin{pmatrix}\Delta x\\ \Delta x'\end{pmatrix}_c=\begin{pmatrix}\sum_{i=1}^{4}\theta_i(s_c-s_i)\\ \sum_{i=1}^{4}\theta_i\end{pmatrix}\quad\text{and}\quad\begin{pmatrix}\Delta z\\ \Delta z'\end{pmatrix}_c=\begin{pmatrix}\sum_{i=1}^{4}\varphi_i(s_c-s_i)\\ \sum_{i=1}^{4}\varphi_i\end{pmatrix}\qquad \text{Eqtn 1}$$

The θ_i should compensate in a closed bump that no angle or displacement error is left. The φ_i are purely parasitic and should be zero at all times.

2.2 Propagation of the injection error

The phase space amplitude excited by the injection process is given by ($y = x$ or z)

$$A_y^2 = \gamma_y (\Delta y)^2 + 2\alpha_y (\Delta y)(\Delta y') + \beta_y (\Delta y')^2 \quad \text{Eqtn 2}$$

with α, β, γ the Twiss parameters at the current location, i.e. at the center of the injection straight. The Twiss parameters always fulfil the relation

$$\beta\gamma = 1 + \alpha^2 \quad \text{Eqtn 3}$$

The amplitude A is an invariant of the betatron oscillation (as long as radiation effects etc. are neglected). Thus the propagation of the injection error to any other location „a" in the lattice is given by the twiss parameter values at these locations. Ignoring betatron phase advances we find for the amplitudes of displacement and divergence at location „a"

$$(\Delta y)_{a,\max} = \sqrt{\beta_{ya}}\ A_y \quad \text{and} \quad (\Delta y')_{a,\max} = \sqrt{\gamma_{ya}}\ A_y\ . \quad \text{Eqtn 4}$$

To neglect nonlinear betatron motions is justified here, since the amplitudes we consider result from imperfect cancellation of the kicks and thus are rather small.
Since the injection as well as the photon beam emission usually takes place at symmetry points of the lattice, i.e. at locations where the beam has a waist (α = 0) we simplify and combine eqtns 2–4 in order to relate the maximum displacement or divergence of the beam at a location „a" to the injection error from Eqtn 1:

$$(\Delta y)_{a,\max} = \sqrt{\frac{\beta_{ya}}{\beta_y}}\ \sqrt{(\Delta y)^2 + \beta_y (\Delta y')^2} \quad \text{and} \quad (\Delta y')_{a,\max} = \sqrt{\frac{1}{\beta_y \beta_{ya}}}\ \sqrt{(\Delta y)^2 + \beta_y (\Delta y')^2}\ .$$

2.3 Multiturn injection error

If the duration of the injection bump T_{bump} is longer than the revolution time of the machine T_{rev} several kicks of different amplitude and at different betatron phases combine to the residual betatron amplitude after termination of the bump.

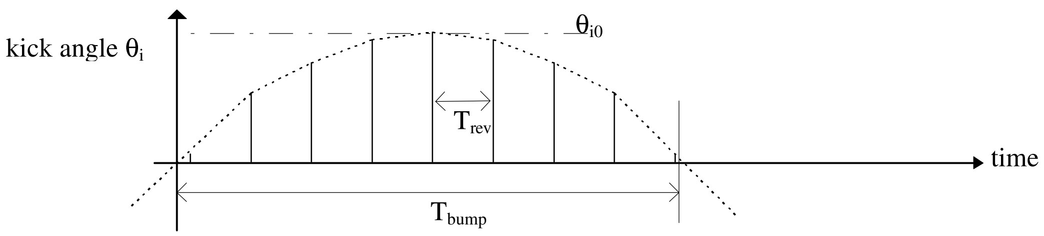

Fig. 5 Half sine kicker bump, extending over several turns

The horizontal kick angle at passage k (with $k = 0$ indicating the crest of the bump) is given by $\theta_{ik} = \theta_i\ (k\ T_{rev}) = \theta_{i0}\ f(k\ T_{rev}) = \theta_{i0}\ f_k$, with $f(t)$ the time function of the bump.

The vertical kicks φ_i have the same time dependancy if they are a constant fraction of the horizontal kicks. This is most likely if they are caused by kicker roll errors.

A common time function is a half sine pulse of duration T_{bump} as shown in fig. 5:

$$f(t)=\cos\left(\pi\frac{t}{T_{bump}}\right),\ \left|t\right|\le\frac{T_{bump}}{2}\quad\text{or}\quad f_k=\cos\left(\pi\,k\frac{T_{rev}}{T_{bump}}\right),\ \left|k\right|\le N=:\left[\frac{T_{bump}}{2\,T_{rev}}\right]\qquad\text{Eqtn 5}$$

Outside the interval T_{bump} the function is zero.
The residual phase space vector after termination of the bump is given by

$$\Delta\vec{y}=\Delta\vec{y}_N+M_y\left(\Delta\vec{y}_{N-1}+\ldots+M_y\left(\Delta\vec{y}_{-(N-1)}+M_y\,\Delta\vec{y}_{-N}\right)\ldots\right)$$

with M_y the one turn matrix of the storage ring lattice at the location of the injection:

$$M_y=\begin{pmatrix}\cos\mu_y+\alpha_y\sin\mu_y & \beta_y\sin\mu_y\\ -\gamma_y\sin\mu_y & \cos\mu_y-\alpha_y\sin\mu_y\end{pmatrix}\ \text{with}\ \ \mu_y=2\pi\nu_y\qquad\text{Eqtn 6}$$

and ν_y the betatron tune of the machine.
Assuming that the time function is exactly the same for all four kickers, i.e. neglecting the time skew and errors in current tracing, we can relate the total kick vector after termination of the bump to the kick vector applied to the beam at the crest of the bump at „turn 0", where the injected beam comes in.

$$\Delta\vec{y}=\Delta\vec{y}_0\sum_{k=-N}^{N}M_y^{N-k}f_k\qquad\text{Eqtn 7}$$

Since a storage ring is a periodic structure the matrix for m turns is the m^{th} power of the one turn matrix and looks exactly like Eqtn 6, but with the m-turn phase advance $m\mu$ replacing the one turn phase advance μ. Exploiting this feature we find for the residual betatron amplitude from inserting Eqtn 6, 7 into Eqtn 2 after some algebra, using Eqtn 3:

$$A_y^2=\left[\left(\sum_{k=-N}^{N}\cos(N-k)\mu_y\,f_k\right)^2+\left(\sum_{k=-N}^{N}\sin(N-k)\mu_y\,f_k\right)^2\right]A_{y0}^2.$$

We eventually obtain for the attenuation or enhancement factor S_y for the residual multiturn betatron amplitude A_y compared to the „turn 0" amplitude Ay_0, as given in Eqtn 2:

$$S_y=:\frac{A_y}{A_{y0}}=\sqrt{\sum_{k=-N}^{N}f_k^2+2\cdot\sum_{k=-N}^{N}\sum_{l=k+1}^{N}f_k\,f_l\,\cos(k-l)\mu_y}\qquad\text{Eqtn 8}$$

This factor is shown in figure 6 with the half sine time structure from Eqtn 5 for several values of T_{bump}/T_{rev} as a function of the betatron tune ν_y. For $T_{bump}/T_{rev}<2$ only one kick is observed and S_y stays at unity, as it is obvious from figure 5. For large values of T_{bump}/T_{rev} the series of kicks interferes destructively as long as the machine tune is not close to an integer. For a given betatron tune we find optimum values of the bump duration, where the residual amplitude is exactly zero, as shown in fig. 7, complementary to fig. 6.
Propagation of the injection error to another location „a" in the lattice was given by Eqtn 4. Inserting the kicker error at the bump crest and multiplying by the factor S_y taking into account the multiturn injection process we finally get for the amplitudes of beam displacement and divergence at location „a":

$$\left.\begin{aligned}(\Delta x)_a&=\sqrt{\beta_{xa}}\\(\Delta x')_a&=\sqrt{\gamma_{xa}}\end{aligned}\right\}\cdot\sqrt{\gamma_x\left(\sum_{i=1}^{4}\theta_{i0}(s_c-s_i)\right)^2+2\alpha_x\left(\sum_{i=1}^{4}\theta_{i0}(s_c-s_i)\right)\left(\sum_{i=1}^{4}\theta_{i0}\right)+\beta_x\left(\sum_{i=1}^{4}\theta_{i0}\right)^2}\cdot S\,(T_{bump},T_{rev},\nu_x)$$

Eqtn 9

$$\left.\begin{aligned}(\Delta z)_a&=\sqrt{\beta_{za}}\\(\Delta z')_a&=\sqrt{\gamma_{za}}\end{aligned}\right\}\cdot\sqrt{\gamma_z\left(\sum_{i=1}^{4}\varphi_{i0}(s_c-s_i)\right)^2+2\alpha_z\left(\sum_{i=1}^{4}\varphi_{i0}(s_c-s_i)\right)\left(\sum_{i=1}^{4}\varphi_{i0}\right)+\beta_z\left(\sum_{i=1}^{4}\varphi_{i0}\right)^2}\cdot S\,(T_{bump},T_{rev},\nu_z)$$

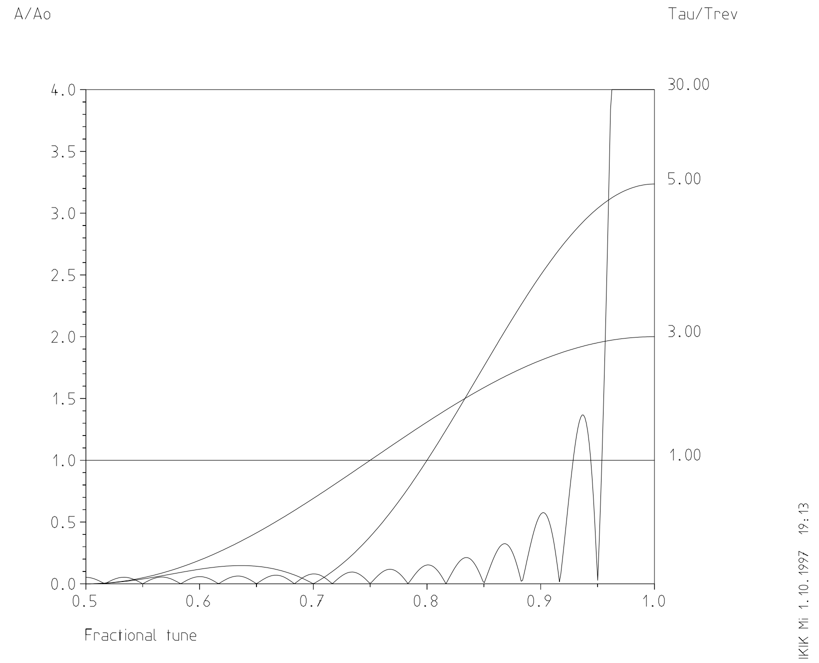

Fig. 6 Ratio of residual betatron amplitude in half sine bump multiturn injection to betatron amplitude in single turn injection as a function of the betratron tune for different ratios of bump duration time over machine revolution time. (The functions in the interval 0...0.5 of betatron tune are just the mirror image of the shown interval shown.)

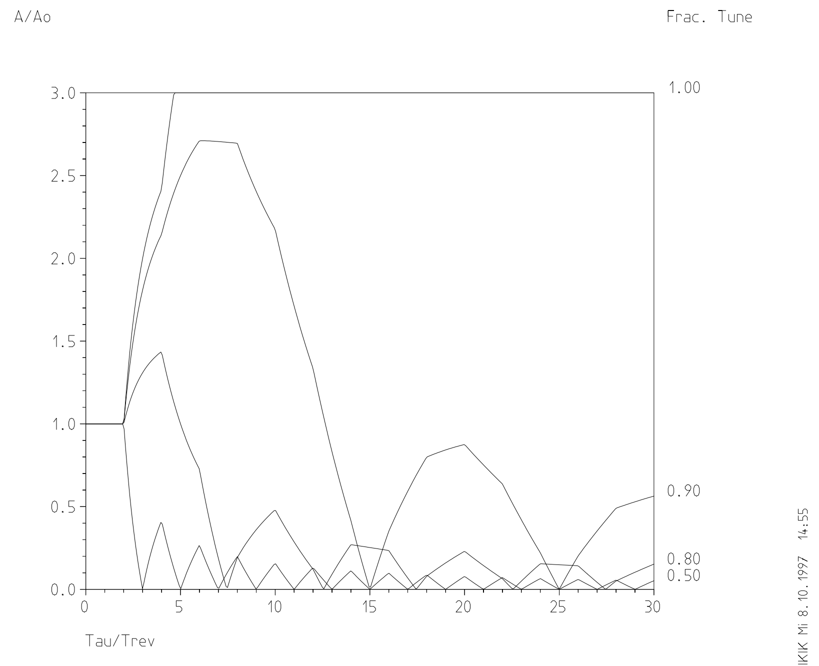

Fig. 7 Ratio of residual betatron amplitude in half sine bump multiturn injection to betatron amplitude in single turn injection as a function of the ratio of bump duration time to machine revolution time for different values of betratron tune. (The kinks in the curves are no artefact from plotting but result from the cut-off of the half sine time function at $\pm T_{bump}/2$.)

2.4 Injection errors for SLS

In order to estimate the acceptable kicker tolerances we will simplify Eqtn 9 and insert numbers for the SLS lattice.
Since X-ray emission as well as injection takes place near centres of straights or dipoles, which are symmetry points of the lattice we set $\alpha = 0$. From Eqtn 3 follows: $\gamma = 1/\beta$.
We further assume for convenience, that all kickers have the same absolute error in kick amplitude $\Delta\theta$, but with most inconvenient polarity in order to get a worst case estimate for the error. Remember that for $\Delta\theta \propto \theta$ the error is zero, because the bump is still closed (see fig. 3).

- If we consider the angle error we find from Eqtn 1 the condition $\theta_1 = \Delta\theta_2 = \Delta\theta_3 = \Delta\theta_4 = \Delta\theta$ to give the worst error of $\Delta x' = 4\Delta\theta$.
- For the displacement error we arbitrarily set $s_c = 0$ and obtain from fig. 1: $s_4 = -s_1 = 5.28$ m, $s_3 = -s_2 = 1.58$ m. The condition to maximize the error is $\theta_1 = \Delta\theta_2 = -\Delta\theta_3 = -\Delta\theta_4 = \Delta\theta$ and gives $\Delta x = 2(s_4+s_3)\Delta\theta = 13.72 \text{ m} \cdot \Delta\theta$.

If the displacement error is maximum the angle error is zero and vice versa. Depending on the betafunction at injection either of them may be the dominating one. Thus we get from Eqtn 9:

$$\left.\begin{aligned}(\Delta x)_a &= \sqrt{\beta_{xa}/\beta_x}\\ (\Delta x')_a &= \sqrt{1/\beta_{xa}\beta_x}\end{aligned}\right\}\cdot \max\{13.72\, m, 4\beta_x\}\cdot S\,(T_{bump}, T_{rev}, \nu_x)\cdot\Delta\theta$$

$$\left.\begin{aligned}(\Delta z)_a &= \sqrt{\beta_{za}/\beta_z}\\ (\Delta z')_a &= \sqrt{1/\beta_{za}\beta_z}\end{aligned}\right\}\cdot \max\{13.72\, m, 4\beta_z\}\cdot S\,(T_{bump}, T_{rev}, \nu_z)\cdot\Delta\varphi \qquad \text{Eqtn 10}$$

These amplitudes remain after termination of the injection process and decay relatively slow by radiation damping.
If we consider only a single kick as error source, e.g. the leakage field of the septum, we simply replace the expression max{...} in Eqtn 10 by the value of β.

Table 1 displays the betafunctions at the centres of the straight sections and at the centre of the TBA center dipole for the SLS lattice in the standard mode as given in the SLS design handbook and also other parameters relevant in the scope of this note.

	SLS standard mode
Long Straight β_x, β_z [m]	3.3 / 6.1
Medium Straight β_x, β_z [m]	2.4 / 1.4
Short Straightβ_x, β_z [m]	1.1 / 1.3
Dipole β_x, β_z [m]	0.4 / 10
Lattice tunes ν_x, ν_z	21.24 / 8.10
Damping times at 2.1 GeV τ_x, τ_x [msec]	12.7 / 13.6
Emittances at 2.1 GeV for 1% coupling ε_x, ε_z [nm rad]	3.1 / 0.03

Table 1 Beta Function Values at Source Region and other Parameters

Injection takes place in a long straight. All straights and the dipole are X-ray source points.

From table 1 and Eqtn 10 we obtain a table of translation factors how the kicker errors cause displacement and angle errors at the source points:

long straight →	$\Delta x/\Delta\theta$ [m]	$\Delta x'/\Delta\theta$	$\Delta z/\Delta\varphi$ [m]	$\Delta z'/\Delta\varphi$
→ long straight	13.7	4.2	24.4	4.0
→ medium straight	11.7	4.9	11.7	8.4
→ short straight	7.9	6.6	11.3	8.7
→ dipole	0.35	11.9	31.2	3.12

Table 2 Factors for transformation of kicker error to source errors

The multiturn factor from Eqtn 8 is not included in table 2. The betatron tunes for the storage ring lattice in standard mode are 21.24 in the horizontal and 8.10 in the vertical. If we assume a half sine bump of 4 µsec duration, we obtain factors $S_x = 1.0$ (equal to unity by chance only) and $S_y = 2.2$ – since the vertical tune is close to an integer, the multiturn effect even aggravates the kicker tolerance problem. With a bump of 6 µsec duration we find $S_x = 0$, i.e. the kicker errors cancel exactly. However it is unlikely that the currents can be controlled so precisely, certainly other error sources, like phase errors, time skew, etc. would become dominant. We neglect the multiturn factor for the rest of this note, optimistically assuming that the lattice is tuned to stay away from integer, and pessimistically assuming that there will be little chance to exploit the multiturn factor successfully.

3. Estimate of Error Requirements for Experiments

An estimate is now made of the beam stability requirements for a "generic" X-ray experiment. To obtain a clear conclusion, the following values are assumed:

- the distance from source to slit (electron beam to experiment) will be 25m (we may already expect that due to this long lever arm the angle errors rather than the displacement errors of the source will dominate the error at the slit);
- X-ray beam widths for dipole and undulator sources are from the SLS Handbook;
- the beam width is conservatively taken as being between the one Standard Deviation points;
- the horizontal and vertical betatron damping times are described by a single exponential decay, with time constants of 13 msec.

Firstly, the static offset errors were assessed. Numerical integration was used to find the intensity of photons with a transverse Gaussian intensity profile passing through a slit, as indicated in Fig.8. The results of the numeric integration are shown in Table 3, for different slit widths.

	Width = →0	**Width = +/- 0.005 SD**	**Width = +/- 0.05 SD**	**Width = +/-0.5 SD**	**Width = +/-5 SD**
Integrated Intensity at Zero Offset	$\frac{w}{\sqrt{2\pi}}$	0.003989	0.03988	0.3831	1.0000

Table 3. Intensity passing a slit of width w with zero offset.

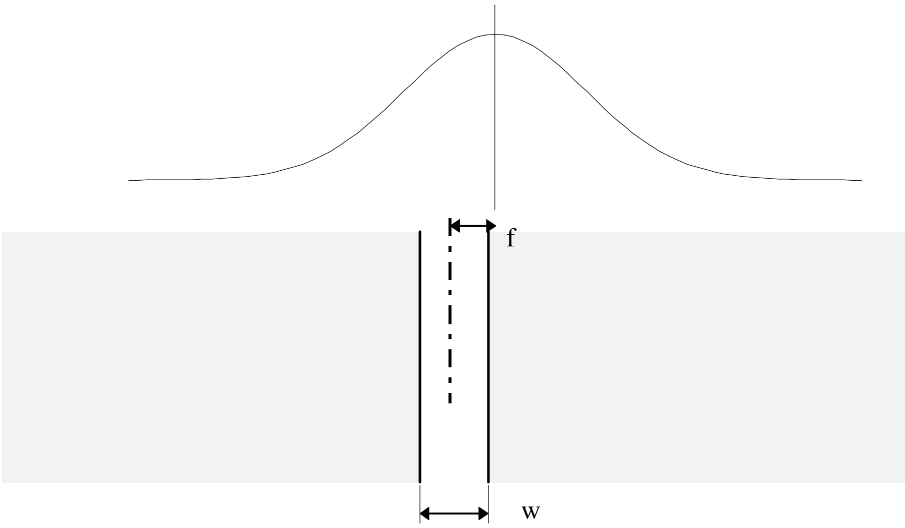

Fig.8 Integrating the intensity passing a slit of width w with an offset f.

Next, the offset values were increased until the intensity was reduced by one bit for different Analog-to-Digital Convertor (ADC) resolutions. The results are shown in Table 4.

	Width = zero	**Width = +/- 0.005 SD**	**Width= +/- 0.05 SD**	**Width= +/-0.5 SD**	**Width= +/-5 SD**
4 bit ADC	$\sqrt{2}\sqrt{2^{-4}}$ SD	0.3593 SD	0.3594 SD	0.3745 SD	3.5315 SD
8 bit ADC	$\sqrt{2}\sqrt{2^{-8}}$ SD	0.08848 SD	0.08851 SD	0.09223 SD	2.4488 SD
12 bit ADC	$\sqrt{2}\sqrt{2^{-12}}$ SD	0.02210 SD	0.02211 SD	0.02304 SD	1.6501 SD
16 bit ADC	$\sqrt{2}\sqrt{2^{-16}}$ SD	0.005524 SD	0.005527 SD	0.005759 SD	0.9913 SD

Table 4. Permitted Beam Offset to Remain Below 1-bit Error

Table 4 shows that the error sensitivity is largely independant of the slit width. From this follows:

a) the experiment ADC resolution is the major factor that determines if a synchrotron light source is found to be "stable";
b) the error sensitivity is largely independant of the source size;
c) the error sensitivity is inversely proportional to source divergence.

These values are conservative, in the sense that a practical 16-bit detector is unlikely to maintain long-term stability below 1-bit error. Table 5 gives values for effective source sizes (including diffraction) from the SLS Handbook:

Source Location	**Dipole** **TBA center**	**Und. 200** **L-straight**	**Und. 38** **M-straight**	**Und.19** **n=1** **S-straight**	**Und.19** **n=11** **S-straight**
Source X	41µm	172µm	80µm	55µm	55µm
Source X'	180µrad	47µrad	42µrad	56µrad	55µrad
Source Z	17µm	138µm	22µm	10µm	6µm
Source Z'	160µrad	38µrad	16µrad	14µrad	12µrad

Table 5. Handbook Values and Estimated Errors for X-ray Sources

Table 6 displays results for the tolerable injection error for different sources, combining numbers from tables 2 and 5. From table 4 we chose the requirement that the beam jitter remains invisible on an 8 bit ADC. This corresponds to the widely „rule of thumb“, that the beam jitter should stay within „10% of sigma“.
Since the point of observation is L = 25 m away from the source, the source size from Table 3 was transformed to the experiment's slit by

$$Y(L) = Y_0\sqrt{1+\left(\frac{Y'_0}{Y_0}L\right)^2} \quad \text{and} \quad Y'(L) = Y_0 . \qquad \text{Eqtn 11}$$

Source	$\Delta\theta$ from Δx [µrad]	**$\Delta\theta$ from $\Delta x'$ [µrad]**	$\Delta\varphi$ from Δz [µrad]	**$\Delta\varphi$ from Δz' [µrad]**
Dipole	1160	**1.35**	11.5	**4.60**
U-200	7.8	**1.00**	3.5	**0.86**
U-38	8.1	**0.77**	3.1	**0.17**
U-19, n=1	16	**0.76**	2.8	**0.14**
U19, n=11	16	**0.75**	2.4	**0.12**

Table 6. Requirements on the maximum kicker errors for the beam jitter to stay below 1 bit on an 8 bit ADC (or to stay within approx. 10% of sigma)

Due to the long lever arm from source to experiment the angle errors are far more severe than the displacement errors. The worst case is found for the mini gap undulator U-10 operating at the 11^{th} harmonic and sitting in a short straight sections. However for other sources, even for the dipole, the situation is not much better.
Kicker magnets with 4.1 mrad deflection would have to match within
0.75 µrad / 4.1 mrad = $\pm 1.8 \cdot 10^{-4}$ (0.018%) in the x-direction and be within $3 \cdot 10^{-5}$ (0.003%) of zero in the z-direction. The situation is no better for the septum magnet with 5^o deflection; the septum leakage field would have to be ±2.9 µrad as well, roughly **0.003 %** of its nominal field strength.
These tolerance requirement, which are already very tough and unlikely to be met, would aggravate by a factor 16 if an ADC of 16 bit instead of 8 bit is considered.

4. Transient offset errors

When top-up injection occurs, the beam is given a closed orbit kick is both the horizontal and vertical planes. It is assumed that no X-rays at all pass the slit during this period. If the kickers could not meet the tolerance requirements given above, we are now interested in the „dead time" for the experiment until the beam has returned to its original position within the resolution of the ADC through radiation damping. The exponential decay is given by:

$$a \le A e^{-t/\tau} \quad \Rightarrow \quad t \ge \tau \ln\left(\frac{A}{a}\right) \qquad \text{Eqtn 12}$$

where a is the tolerance limit, A is the amplitude of the initial disturbance and τ is the damping time constant.

- Anticipating the next section we assume kicker errors of 0.35 %, i.e. A = 14 μrad for a 4.1 mrad kicker);
- For the tolerance limit a we use the worst case value from table 6, i.e. 0.12 μrad for U-19 on the 11th harmonic;
- The damping time τ is approx. 13 msec from table 1.

With these example values, the decay time is a maximum of 62 msec with 8 bit ADC and 98 with 16 bit ADC respectively. During this interval the data acquisition would be disabled.

5. Error Factors from Magnetic Field

For a general magnetic path through a dipole, the integrated field strength is

$$\int B dl = \mu_o \left[\frac{1}{\dfrac{G(\mu_r)}{\mu_r(t)} + g(t)} \right] N\left[I(t) + I_R + I_e(t)\right] l_e(t)$$

where:

$\mu_o = 4\pi \times 10^{-7}$
μ_r = mean iron permeability
G = mean flux path in iron
g = mean air gap
N = number of turns
I(t) = coil current
I_R = equivalent remanence current
Ie(t) = equivalent eddy current effect
l_e = effective length of magnet

With the novel requirement for matching the kicker fields to high precision, each one of the above factors must have error tolerances. Since the error contributions from the four magnets are not identical, it is not sufficient to note differenential changes between magnets - absolute changes are required. These values are estimated without a scrap of experimental data:

$\Delta\mu_r$ = +/-5% for non-uniformity of rolled steel,
-1%/°C over 10°C = -10% for change of permeability with temperature,
+/-5% due to insulation thickness.

ΔG = +/-1% as a result of localised non-linear flux redistribution

Δg = +20ppm/°C over 10°C = +0.02% (+2.4μm) due to thermal expansion,
-0.038% (-4.5μm) due to magnetic forces,
+/-0.05% due to magnetostriction
ΔN = +/-0.1% due to mechanical working of coil fixations
$\Delta I(t)$ = +/-0.2% average, but a function of time, inductance, capacitance, switch (with considerable engineering effort)
ΔI_R = +/-10A due to non-uniformity of magnetic grain size in steels between the four magnets
ΔI_e = +/-10A due to non-uniformity of lamination thickness, magnetic grain size and packing factor in steels between the four magnets
Δl_e = +20ppm/°C over 10°C = 0.02% due to thermal expansion

Collecting these factors gives a worst-case value of +/-0.35%. The power supply variations remain a dominant factor.

6. Error Factors from Magnet Alignment

The magnetic field in each of the four kickers will not be perfectly normal to the electron beam. This alignment error has nothing to do with geodetic measurement errors, but rather due to the variable permeability of the magnet ferrite and the uncontrolled end fields; these errors are relatively large because the magnet is small.

There are three axes (x, z and s) of rotation (pitch, yaw and roll) and of displacement (sway, heave and surge). An approximation may be developed in a later Note for the effect of the end fields. For the moment, these are only noted:

Yaw (rotation about the z-axis)
This gives a tiny increase in path length through the magnet, and probably a tiny reduction in the end field. The field lines remain perpendicular to the electron beam.

Pitch (rotation about the x-axis)
This gives a tiny reduction in the vertical component (the longitudinal component is not seen by the beam),

$$\Delta\theta_i = \theta_i(1-\cos\alpha)$$

where α = the magnet alignment error (eg 2mrad)
θ = the nominal magnet deflection (eg 4.1mrad)

Roll (rotation about the s-axis)
Roll introduces a large horizontal field component, as shown in Fig.9, deflecting the beam vertically. This error is unique because it is independant of end fields.

$$\Delta\varphi_i = \theta_i \sin^{-1}(\alpha) \approx \theta_i\alpha$$

Surge (displacement along the s-axis)
A displacement of the magnetic centre along the electron beam axis. The effect is to give a horizontal offset the electron beam by

$$\Delta s \tan\theta_i = \Delta x$$

where Δx = offset parallel to the beam axis
θ_i = mean value for the magnet deflection (eg 4.1mrad)

Δs = surge displacement (eg 1mm)

Heave (displacement along the z-axis)
The errors come from end fields only. This gives a tiny reduction in the vertical component (the longitudinal component is not seen by the beam).

Sway (displacement along the x-axis)
The errors come from end fields only. Unlike yaw, the end field errors may add, and may be of the order of 0.1% for 1mm sway.

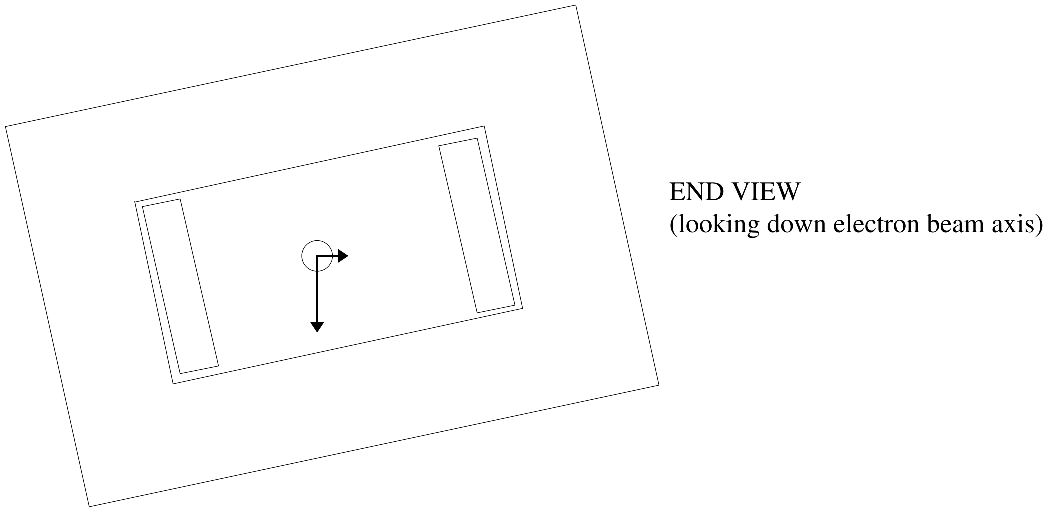

Fig.9 Roll (Axial Rotation) Error

7. Choice of Reference Waveform

<u>If</u> a precision method is found to measure the magnet currents, it is then necessary to define what each waveform should be compared against. The difference between the measured waveform and the reference waveform gives the sign of the error, and also is easier to implement with precison linear analog electronics.

With the Angle Error dominant, then the reference waveform could be the simple average,

$$\theta_{ref}(t) = \frac{(\theta_1(t) - \theta_2(t) - \theta_3(t) + \theta_4(t))}{4}$$

where the negative signs appear because of the choice of signed angles. The errors could be the deviation from the average,

$$\Delta\theta_i = \theta_i - \theta_{ref}$$

In this case, the reference waveform could be treated as exact, and the current measurement precision would need to be, say, 0.1%.

8. Summary and Conclusion

- For any source, the permitted Source Angle Error is more sensitive than the permitted Source Displacement Error for injection magnet errors.

- For undulator sources, the injection magnets should each have errors of **0.018 %** in the x-direction and be within **0.003 %** of zero in the z-direction to give no measureable disturbance to an 8-bit ADC.

- The septum leakage field would have to be **<0.003 %** of its nominal field strength to give no measureable disturbance to an 8-bit ADC.

- A guess at a practical minimum that can be achieved with kicker technology is ±0.35%, or ±14µrad.

- An estimate of the alignment errors show that Roll (longitudinal rotation around the electron beam axis) is a problem. This introduces relatively large vertical errors, eg 1mrad Roll would give 4µrad error at an X-ray source.

- The settling time (experiment outgated) for the kicker errors to decay below the resolution of the 8 [16] bit ADC is 62 [98] msec.

- Interferences between successive turns in slow bumps may significantly reduce the residual injection error. On the other hand errors are amplified if the lattice tune is close to an integer.

Conclusion: The beam jitter from kicker errors will be visible to the experiment in any case. Thus top-up injection may only work with gated data acquisition.

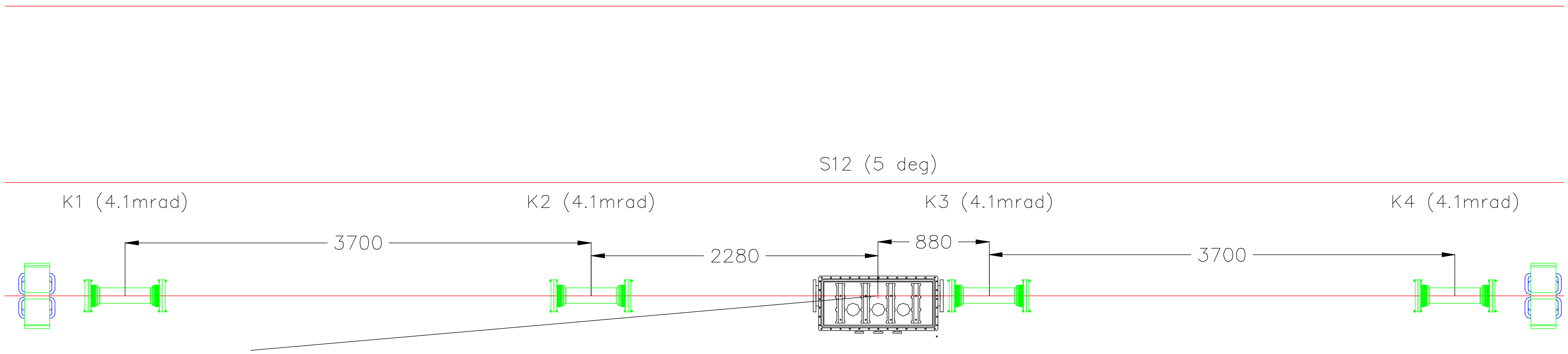

Fig.1 Storage Ring Injection Configuration